Proceedings of the XVII ECSMGE-2019
Geotechnical Engineering foundation of the future
ISBN 978-9935-9436-1-3

doi: 10.32075/17ECSMGE-2019-0273

XVII European Conference
ECSMGE 2019
Reykjavik
on Soil Mechanics
and Geotechnical Engineering

Experimental study of dry and semi-submerged scaled geotechnical models subjected to seismic loading, incorporating monitoring techniques

Étude expérimentale de modèles géotechniques de talus, secs et semi-submergésétudiés à l'échellesoumis à des charges sismiques,intégrant de techniques de surveillance

E. Kapogianni
National Technical University of Athens, Greece
S. Tsafou, M. G. Sakellariou
National Technical University of Athens, Greece

ABSTRACT: The purpose of this study is to investigate the behaviour of scaled geotechnical models subjected to seismic loading. The experimental models have been tested on the APS 400 Electro-Seis force generator of the National Technical University of Athens, incorporating various measuring techniques. A total of 8 slope models were built and studied, with a variety of specific characteristics and in particular (a) dry or semi-submerged, (b) with steep or minor slope inclination, (c) unreinforced or incorporating soil reinforcement, and (d) incorporating a pipe in order to simulate a scaled pipeline. Optical fibre sensors have been placed at various locations inside the slope models in order to record strains during the application of the seismic loading. In addition, the Digital Image Correlation technique has been applied on the side face of the models in order to capture the failure mechanisms. Furthermore the acceleration levels have been recorded via an accelerometer located on the base of the force generator. The model making procedure and test set up are presented as well as recordings, focusing in parallel on the effect of the water on the stability of the models and the failure mechanisms.

RÉSUMÉ: Les modèles experimentaux ont été testés sur le générateur de force APS 400 Electro-Seis de l'École polytechnique d'Athènes, integrant diverses techniques de mesure. Un total de 8 modèles de sable on tété construits et étudiés, avec une variété de caractéristique sspécifiques telles que: a) sec ou semi-submergé, b) avec une pente raide ou mineure, c) incorporantou non un renforcement du sol, d) incorporant un pipeline afin de simuler un pipeline mis à l'échelle. Des capteurs à fibres optiques ont été placés à divers emplacements sur les modèles de talus afin de consigner les deformations lors de l'application du chargement sismique. Enoutre, la technique de correlation d'image numérique appliquée sur la face latérale des modèles a permis de cibler les différents mécanismes de défaillance. Les niveaux d'accélération ont étéenregistrés via un accelerometer situé à la base du générateur de force APS. La procédure de création du modèle et la configuration de tests ainsi que les enregistrements via les techniques susmentionnées sontprésentés du; une attention particulièreestportée sur l'impact de l'eau sur les mécanismes de stabilité et de défaillance modèle.

Keywords: physical modelling in geotechnics; seismic loading; smart monitoring, optical fibres; image analysis

1 INTRODUCTION

The trigger for this study is the continuous and worldwide development of energy networks. Lifelines in the modern world are part of the national wealth of each country, and the need for continued research and development is now imperative. In this framework, physical modelling of scaled slope models has been performed, aiming to the investigation of their behavior due to seismic loading conditions. In order to achieve this goal, several scaled models have been built and tested, in order to provide reference experiments for comparison (Finno, 2014; Laue, 2014; Springman, 2014).

2 MATERIALS AND EQUIPMENT

In this section the laboratory equipment is described and more specifically (a) the Force Generator used for the loading impose and the Amplifier, (b) the Data Acquisition Card and the LabView software for the system operation (c) the QCN Sensor for real-time recordings of the acceleration applied, (d) the Optical Fiber Sensors, and (e) the Digital Camera used for the image correlation technique application.

2.1 Force Generator and Amplifier

In Figure 1 the Electro Seis one degree of freedom force generator used to create seismic motion to the models by converting the electrical signal into kinetic energy is shown. Furthermore, the amplifier used to convert the low-power supply signal to a signal suitable for direct movement of the shaker can be seen (APS Dynamics, 2014).

Figure 1. APS 400 ELECTRO-SEIS Force Generator and EP-124 Amplifier

2.2 NI Card and LabView

The NI USB-6009 (Figure 2) is a data acquisition card with analog and digital inputs and outputs and has been used for the connection of the computer to the generator in order to achieve control of the frequency and magnitude of shaking table. In addition, a software in LabView environment has been used for the control of the generator.

Figure 2. NI USB-6009 Card

2.3 QCN

The Quake-Catcher Network is a collaborative initiative that aims to develop the world's largest, low-cost, powerful seismic network, using sensors connected to Internet-connected computers (QCN, 2016). The sensor used in the current experimental layout is noted in Figure 3 and has the advantage of measuring the acceleration in 3 axial directions.

Figure 3. QCN acceleration sensor

2.4 Optical Fibre Sensors

A Fiber Bragg Grating (FBG) sensor is an integral special treated optical fibre portion, with the ability to act as an optical filter to incoming radiation, reflecting a minimal amount of wideband light signal. This modified area is sensitive to tensile stress, compression and changes due to temperature alterations so that the wavelengths reflected change accordingly. Optical fibre sensors combine precision (microstrain) with resistance to mechanical stress and multiplexing of signals (FOS&S, 2008; SmartFibres, 2008). An important advantage is that they can be placed on various positions, due to their adjustable size, on almost any structure or experimental model, in small or larger scale (Kapogianni et al, 2010a; Kapogianni et al, 2017). In Figure 4 the strain FBG sensors that have been used in the experimental set up of the current study can be seen. The connections of sensors were made possible in various ways, either with the use of the appropriate adhesive, or with the use of coating for protection or attached directly to the into geotextiles, for the case of the reinforced slope models.

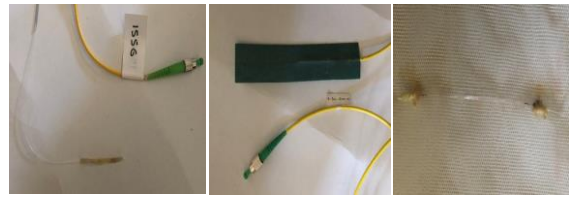

(a) *(b)* *(c)*

Figure 4. FBG sensors (a) unrestrained, (b) with sheathing, (c) in geotextile

2.5 Digital Camera

For the test set-up and in order to apply the image analysis method (Kapogianni et al, 2010b), an action camera has been used. The camera selected had a small weight and was placed on the platform of the shaking table, with the use of support mechanism, in order to follow the movements of the models during the seismic loading. Furthermore, the wide-angle len of the camera made it possible to record the entire surface of the models from short distance.

2.6 Soil Material

The soil material used for model construction was a non cohesive white sand with internal friction angle of 35°. The models were built inside a rigid and watertight box made of Plexiglass. Even though the soil material used was non cohesive, it developed a low cohesion due to water presence. For the determination of this cohesion a penetometer has been used (Tsafou, 2018).

3 PHYSICAL MODELLING

For the current study, 8 scaled slope models were built inside a rigid and sealed box made of Plexiglass, fixed on a wooden base. The geometry of the Plexiglass box was 50 cm (length) x 30 cm (width) x 22 cm (height) and the box weight 5.7 kg. Optical fibres were incorporated into the models and strain measurements were made possible. More specifically the sensors were placed either

without restrains or attached to scaled geo-textiles. Models of similar geometry and features were tested and shown in what follows.

3.1 Dry Slopes

Two dry scaled slope models with similar geometry were built and tested at the APS shaking table, incorporating an optical fibre sensor at two different positions. The characteristics of each model, the acceleration levels and the maximum strain developed are shown in Table 1 and the experimental layout in Figure 5. To be able to stabilize the model a predefined small amount of water was added layer for layer throughout the construction to provide suction. This first set of the tests aimed to the investigation of the model making procedure and the development of the tests set-up, including the strain optical fibre data acquisition and acceleration recordings.

For the first model the optical fibre sensor was attached on a geotextile, placed at the bottom of the box / slope model, while for the second model the optical fibre sensor was attached on a geotextile, 4 cm above the box / slope model bottom (Figure 6).

Table 1. Test No.1 and Test No.2

Test No.	1	2
Acceleration	3.4 m/s^2	2.8 m/s^2
Slope Characteristics	B=30cm β=8cm h=15cm α=34^o	B=30cm β=7cm h=18cm α=38^o
O.F. Elevation	0 cm	4cm
FBG strain	6 μstrain	2 μstrain

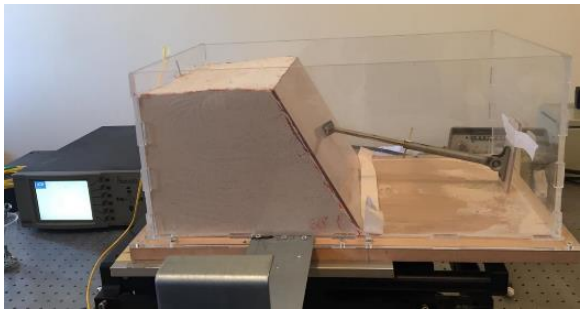

Figure 5. Experimental layout and slope model

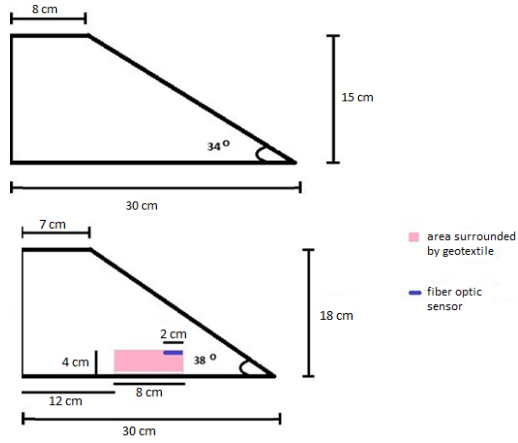

Figure 6. Side view of Tests No. 1(top) & 2 (bottom)

3.2 Semi-Submerged and Dry Slopes

Furthermore, the influence of water on the models has been examined and a comparison of dry and semi-submerged slopes with similar geometry has been made (Figure 7). The water level at the semi-submerged models was at 4 cm and an optical fiber sensor has been incorporated.

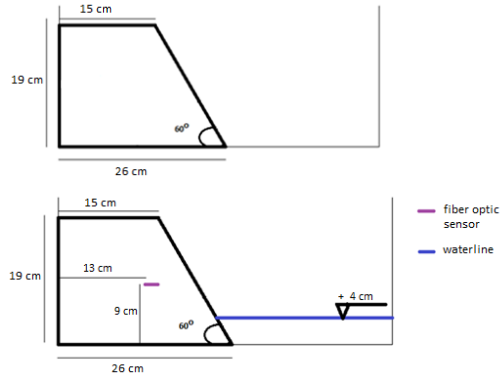

Figure 7. Side view of Tests No. 3 (top) & 4(bottom)

In Figure 8 the failure mechanisms of the two slope models are presented after seismic loading impose. It is noted that the presence of water affects the behaviour of the slope and the failure scheme, due to sunction and also due to the development of subsoil on the surface adjacent

to the free water level. On the other hand, the dry slope suffers from non-circular rotational sliding.

Figure 8. Failure mechanisms during Tests No. 3(left) and 4 (right)

In Table 2, the geometrical and mechanical characteristics of the modes are shown, the loading conditions and the maximum strain recorded via the optical fibre sensor for the semi-submerged slope. The influence of water on the reduction of the slope strength was expected since the rise in water level entails an increase in the water pressure of the pores and a corresponding decrease in the shear-strength of the saturated slope material.

Table 2. Test No. 3 and Test No. 4

Test No.	3	4
Acceleration	3.6 m/s^2	2.85 m/s^2
Slope Characteristics	B=26cm β=15cm υ=19cm α=60^o	B=26cm β=15cm υ=19cm α=60^o
Water Level	dry slope	4cm
FBG strain	(No sensor)	450 μstrain
Failure Mechanism	Non-circular swiveling slide	Overturning pieces

In Figure 9, strain recordings via the optical fibre sensor for Test No.4 are shown, while the slope is submitted to seismic loading. As expected strains increase during seismic loading increment and the higher strain values occur at slope failure.

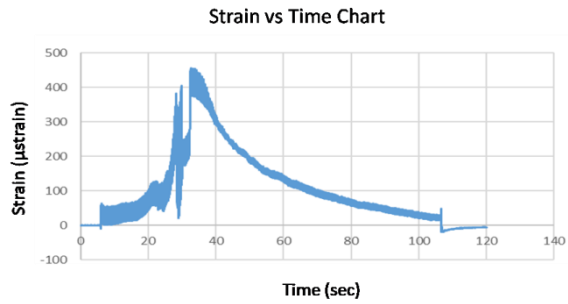

Figure 9. Strain versus Time Chart, during Test No4

Furthermore, analysis with the Digital Image Correlation (DIC) technique with the use of Vic2D software (Correlated Solutions, 2009)was performed for the semi-submerged model. More specifically digital images were captured during different phases of the model loading procedure and indicative results are shown in Figure 10, including the failure mechanism in progress. More specifically strain localization is observed, before the overal failure, a phenomenon characteristic for granular materials. Strain localization is of considerable practical significance, since the stability and deformation characteristics of the soil structures are often controlled by the soil behavior within the shear zones.

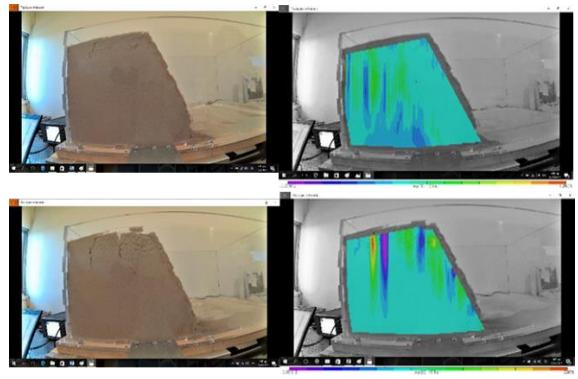

Figure 10. Snapshots of the semi-submerged slope during seismic loading (left) and shear strain field (right)

3.3 Semi-submerged slopes incorporating a model pipe

In the following two models (No. 5 and No. 6) with the same geometry and water levels are presented (Figure 11), both incorporating an optical fibre sensor attached on a pipe, in order to simulate the behaviour of a scaled pipeline, inside a slope model. Test No. 5 was built by compressing the soil material, while model No. 6 was built via dry deposition of the sand (pluviation). In Table 3 the geometrical characteristics of the models, the acceleration levels, the construction method and strains recorded via the optical fibre sensors are shown.

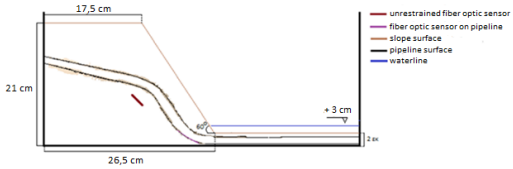

Figure 11 Side view of Test No.4 and Test No.5

Table 3.Test No. 5 and Test No. 6

Test No.	5	5	6	6
Acc	2.6 m/s^2	3.1 m/s^2	2.6 m/s^2	3.0 m/s^2
Slope Characteristics	B=26.5cm β=17.5cm h=21cm α=60°	B=26.5cm β=17.5cm h=21cm α=60°	B=26.5cm β=17.5cm h=21cm α=60°	B=26.5cm β=17.5cm h=21cm α=60°
Water Level	3 cm	3cm	4.5 cm	4.5 cm
Construction Method	compression	compression	pluviation	pluviation
FBG (pipeline)	10 μstrain	15 μstrain	120 μstrain	140 μstrain

It is noted that strains recorded during Test No. 5 are significant smaller than the corespondent strains recorded during Test No.6. This is attributed to the different construction method, i.e. compressed soil for Test No. 5 and dry deposition of the soil material (pluviation) for Test No.6. In Figure 13, acceleration levels and strains for Test No. 6, are shown, as recorded during the seismic loading procedure.

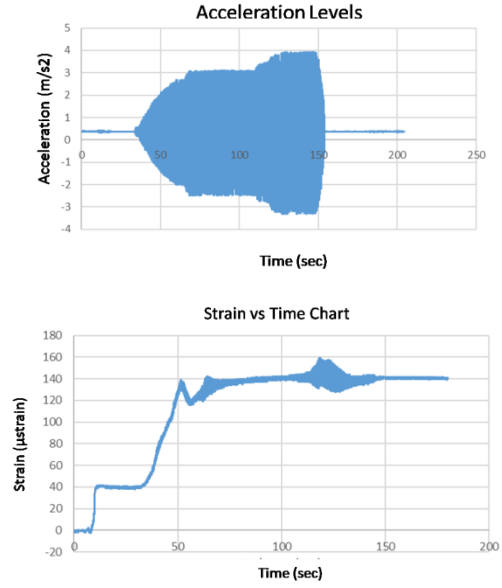

Figure 13. Acceleration Levels (top) and Strains (bottom) versus Time Chart, during Test Test No. 6

In addition, the Digital Image Correlation (DIC) technique was applied and strains and failure mechanisms have been defined. Indicative results are shown in Figures 14 and 15 for Test No. 5 and Test No. 6 respectively. It should be mentioned that no strain localization phenomena have been observed during these two tests, which is attributed to the presence of water.

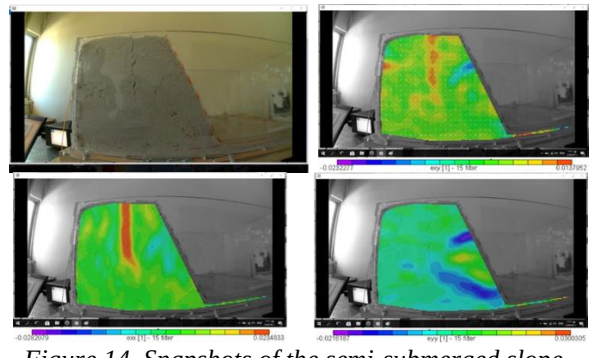

Figure 14. Snapshots of the semi-submerged slope for Test No. 5 and strain fields

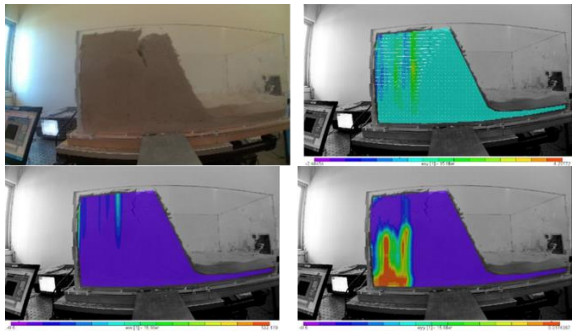

Figure 15. Snapshots of the semi-submerged slope for Test No. 6 and strain fields

3.4 Steep Reinforced Models Dry and Semi-Submerged

The final set of tests concern steep reinforced slope models (Koerner, 2015) with identical geometrical characteristics and acceleration levels (Fig. 16). More specifically the model for Test No. 7 is dry and the model for Test No. 8 is semi-submerged. Two sensors were attached on each model, connected in series. The rest of the model characteristics are noted in Table 4. It should be noted that for Test No. 7 no failure has occurred, while for Test No. 8 the water presence has contributed to slope failure and higher strains recorded via the optical fibres. This failure mechanism is also reflected in Figures 17 and 18, where the original and final state of the semi-submerged model is shown (Fig. 17) and the results occurred after the DIC analysis (Fig. 18). In addition, the phenomenon of the local strain localization is also present.

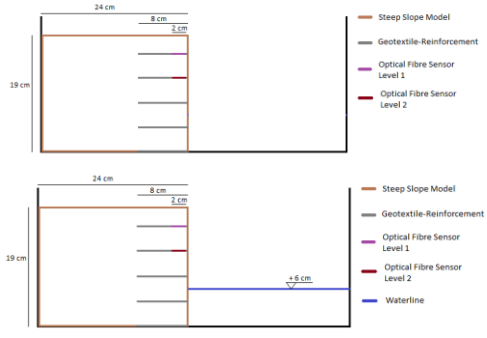

Figure 16. Side view of Test No.7& Test No. 8

Table 3. Test No. 7 and Test No. 8

Test No.	7	7	8	8
Acceleration	3.0 m/s^2	4.0 m/s^2	3.0 m/s^2	4.0 m/s^2
Geometry	Vertical Slope			
Water	Dry Slope	Dry Slope	Submerged Slope	Submerged Slope
FBG (1st layer)	8 μstrain	11 μstrain	650 Mstrain	20 μstrain
FBG (2nd layer)	4 μstrain	6 μstrain	32 μstrain	30 μstrain

Figure17.Snapshots of the semi-submerged, vertical slope failure (Test No. 8)

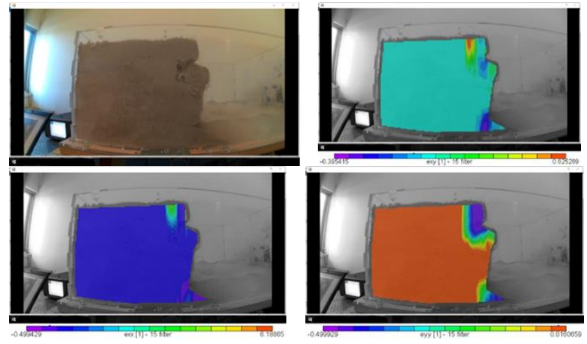

Figure 18. Strain fields (Test No. 8)

4 CONCLUSIONS

In the current study, several scaled sand slope models with various characteristics (i.e. unreinforced, reinforced, incorporating a pipe, dry or semi-submerged), were built and tested at a one degree of freedom APS force generator. Optical fibre sensors were incorporated inside the models and the effect of water presence was investigated. Furthermore, the Digital Image Correlation (DIC) technique was applied, via the software Vic2D and the failure mechanisms were captured.

Concerning the dry slope model, the failure was due to slip of the soil material, as expected for a non-cohesional soil and the failure zone was developed alongside the incline of the slope. For the semi-submerged slopes, it was noted that the presence of water affected the behaviour of the models and the failure mechanisms, due to sunction and also due to the development of subsoil on the surface adjacent to the free water level.

Furthermore, optical fibre measurements were made possible for dry and for semi-submerged models and variations on the recordings were noted, related to the specific characteristics of each model.

Regarding the investigation with the DIC technique, strain localization phenomena were captured, and the failure mechanisms were defined.Furthermore, this method enabled us to look at the behaviour of the models prior to failure, bu capturing the concentration of strains.

Concluding, the test set-up and techniques used can be applied in models with various characteristics, possible other than slopes, providing a comprehensive view of their behaviour.

5 REFERENCES

APS Dynamics, 2014. APS 400, Electro Seis Manual.

Correlated Solutions, 2009. Vic2D Manual.

Finno, R.J., 2014. Performance Monitoring of Geotechnical Structures, September-October. Geostrata, 14-16.

FOS&S, 2008. Strain Gage Installation Kit SGK-01.

Kapogianni, E., Sakellariou, M.G. & Laue, J., 2017. "Experimental Investigation of Reinforced Soil Slopes in a Geotechnical Centrifuge, with the Use of Optical Fibre Sensors", Geotechnical and Geological Engineering, Vol. 35 (2), pp. 585-605.

Kapogianni, E., Laue, J., Sakellariou, M. & Springman, S.M., 2010a. The use of optical fibers in the centrifuge, 7th International Conference on Physical Modelling in Geotechnics, Zurich, Switzerland.

Kapogianni, E., Laue, J. & Sakellariou, M., 2010b. Reinforced slope modelling in a geotechnical centrifuge, 7th International Conference on Physical Modelling in Geotechnics, Zurich, Switzerland.

Koerner, R.M., 2005. Designing with Geosynthetics. 5th Edition.

Laue, J., Springman, S.M., Gautray, J., Morales, W.F., Iten, M. & Arnold, A., 2014. 15 years of experience using a physical model exercise in a Masters' course. Proceedings of the 8th International Conference on Physical Modelling in Geotechnics, Perth, Australia, 445-450.

National Instruments Corporation, 2003. LabView User Manual.

SmartFibres, 2008. SmartSoft V3.2.0.

Springman, S.M., Laue, J., Herzog, R. & El-Hamalawi, A., 2014. The evolution of a physical modelling course over two decades. Proceedings of the 8th International Conference on Physical Modelling in Geotechnics, Perth, Australia, (1) 433-439.

Tsafou, S., 2018. Experimental and Numerical Investigation of The Seismic Response of Dry and Semi-Submerged Slopes. MSc. Thesis, National Technical University of Athens.

http://qcn.stanford.edu